Available online at www.sciencedirect.com
SCIENCE DIRECT®
Journal of the European Ceramic Society 25 (2005) 1025–1031
www.elsevier.com/locate/jeurceramsoc

The resistance to oxidation of an HfB_2–SiC composite

Frédéric Monteverde*, Alida Bellosi

Institute of Science and Technology for Ceramics, National Research Council, Via Granarolo 64, 48018 Faenza, Italy

Received 12 March 2004; received in revised form 12 May 2004; accepted 15 May 2004
Available online 22 July 2004

Abstract

The oxidation resistance of an hot-pressed HfB_2–SiC composite was studied through non-isothermal and isothermal treatments at temperatures up to 1600 °C in air. The most severe oxidation conditions consisted of repeated heating-cooling cycles at 1600 °C for up to 80 min of exposure. A thermogravimetric test for over 20 h at 1450 °C provided evidence that, at this temperature, the oxidation kinetics fits a paralinear law until 10 h, when a partial rupture of external oxide scale occurs (i.e. a break-away reaction). Afterwards, the weight gain data fit a linear law. The main secondary phases formed in the composite during hot-pressing, namely BN, Hf(C,N) and a Si-based compound, although in limited amounts, influenced the oxidation resistance at temperatures below 1350 °C. At temperatures higher than about 1400 °C, the presence of SiC particles markedly improved the oxidation resistance due to the formation of a protective borosilicate glassy coating on the exposed surfaces.

Keywords: Hot-pressing; Composites; HfB_2; Microstructure; Oxidation resistance; SiC

1. Introduction

Ultra-high temperature ceramics (UHTCs), particularly diborides and carbides of the transition metals like hafnium and zirconium, are currently accepted as potential candidates for a variety of high-temperature structural applications, including furnace elements, plasma-arc electrodes, or rocket engines and thermal protection structures for space vehicles with temperature capabilities at over 1800 °C.[1–3] The growing interest in UHTCs stems from the opportunities they provide for designing a new generation of space vehicles with very sharp leading edges.[4] This innovative class of materials has the potential to overturn an age-old tenet of aerodynamics, that only blunt-body spacecraft can survive the searing temperatures generated as the vehicle repeatedly tears through the terrestrial atmosphere during hypersonic flights. The expected highly localized heating loads in the areas particularly exposed to the interaction with the atmosphere during re-entry missions dictate the need for oxidation and ablation resistance, coupled with a low surface catalytic efficiency, and a capacity to conduct away or re-radiate excess energy.[5] The introduction of SiC in matrices of zirconium and hafnium diborides improved the mechanical properties[1,3,6] and oxidation resistance.[3,7–9]

Existing research activities are still facing technological difficulties in scaling-up the manufacturing of near net-shape dense components. Sintering conditions of elevated temperatures and pressure[3,4] induce coarsening of the microstructure and a general degradation in the mechanical properties. The addition of sintering aids have proven to be a suitable route to improving the sinterability and to controlling development of the microstructure during the densification of refractory diborides matrices.[6,9,10]

The present study deals with an HfB_2–SiC composite (containing 5.8 v/o Si_3N_4 as sintering aid) hot-pressed at 1850 °C for 20 min. The oxidation behavior in ambient air was studied by monitoring the weight change, according to different thermal treatments. Modifications in the microstructure were examined and correlated to the oxidation mechanisms involved.

2. Experimental

2.1. The fabrication of the material

The starting powder mixture, of composition (v/o) $HfB_2 + 19\ SiC + 5.8\ Si_3N_4$, was milled for one day in a

---

* Corresponding author. Fax: +39 0546 463 81.
E-mail address: fmonte@istec.cnr.it (F. Monteverde).

0955-2219/$ – see front matter © 2004 Elsevier Ltd. All rights reserved.
doi:10.1016/j.jeurceramsoc.2004.05.009

Table 1
Thermomechanical properties of the composite: Vickers microhardness Hv1.0, fracture toughness (chevron notch method) K_{iC}, linear thermal expansion coefficient λ, 4-pt flexural strength (at different temperatures) σ

Hv1.0 (GPa)[a]	K_{iC} (MPa$\sqrt{m}$)[a]	λ (10^{-6} °C^{-1})			σ (MPa)[a]			
		25–1000 °C	25–1200 °C	25–1300 °C	25 °C	1200 °C	1400 °C	1500 °C
20.4 ± 0.6	4.3 ± 0.1	7.24	7.37	7.30	560 ± 100	380 ± 50	280 ± 20	150 ± 5

[a] Mean ± 1 S.D.

polyethylene jar using absolute ethanol and silicon nitride balls, and then dried and sieved. The as-processed powder batch was hot-pressed at 1850 °C for 20 min and 30 MPa of applied pressure, using an induction-heated BN-lined graphite die. Some properties of the composite are listed in Table 1. Details concerning the densification behavior, microstructure and thermomechanical properties of the composite are reported elsewhere.[10]

2.2. The oxidation treatments

The composite was subjected to various oxidation treatments (at ambient pressure), namely:

(A) Non-isothermal run up to 1450 °C in flowing dry air (50 cm^3/min), heating rate 2 °C/min and free cooling.
(B) Isothermal runs at 1170 °C, 1250 °C, 1350 °C and 1500 °C for 1 h (loading and removal of the sample at the fixed set-point). After the loading of the test piece, the furnace took up to 10 min to reach the desired temperature.
(C) Isothermal run at 1450 °C for 20 h in flowing dry air (50 cm^3/min), heating rate 30 °C/min and free cooling.
(D) Isothermal runs at 1600 °C for 20, 40 and 80 min of exposure (loading and removal of the coupon at the fixed set-point for each scheduled exposure). After the loading of the test piece, the furnace took 15 min to reach the temperature of 1600 °C.

Coupons with dimensions of 2.5 mm × 2.0 mm × 10.0 mm (for treatments A–C–D) and dimensions of 10 mm × 10 mm × 1 mm (for treatment B) were cut out from the sintered billet (surface finish $R_a \sim 0.2\,\mu m$), washed in an ultrasonic bath of acetone, and dried at 80 °C overnight. Treatments A and C were executed using a thermogravimetric analyzer (mod. STA409, NETZSCH Gerätebau GmbH, Germany) equipped with a vertically heated Al_2O_3 chamber. The samples were placed on zirconia supports, separating them from the Al_2O_3 holder. The mass variation was recorded (10^{-3} mg of accuracy) over the scheduled thermal cycle. Treatments B and D were performed using a bottom-loading furnace box. The test piece was placed upon SiC supports with minimal contact area. The sample mass was measured before and after each cycle.

2.3. The analysis of the microstructure

The microstructure was analyzed with a scanning electron microscope (SEM, mod. S360, Cambridge, UK) equipped with an energy dispersive microanalyzer (EDX, mod. INCA Energy 300, Oxford Instruments, UK), and an X-ray diffractometer (XRD, mod. D500, Siemens, Germany). Sections of some oxidized coupons were first polished using diamond abrasives (finished 0.5 μm), and then observed via SEM-EDX analyses. The cross-sections were imaged using secondary electrons (SEs), free of conductive coating in order to maintain the sensitivity of the EDX equipment to the low Z elements as high as possible. The thickness of the oxidized specimens was measured (accuracy ± 2 μm) using an optical microscope.

3. Results

3.1. The microstructure of the hot-pressed composite

The bulk density of the hot-pressed material was 8.8 g/cm^3. The SEM observations of the fracture surface showed regularly shaped HfB_2 grains, 5 μm maximum in size, and SiC particles (Fig. 1). In addition, other (crystalline) phases were detected by XRD analysis: monoclinic HfO_2 and a cubic Hf(C,N) solid solution. The SEM-EDX examination of the polished section identified all the mentioned phases, but also highlighted some more minority compounds formed during hot-pressing, basically an Si-based phase and boron nitride, which are all located intergranularly (Fig. 2). EDX spectra from the main secondary phases are shown in Fig. 3. The SiC particulate, which represents the majority of the dark features in Fig. 2, is partly

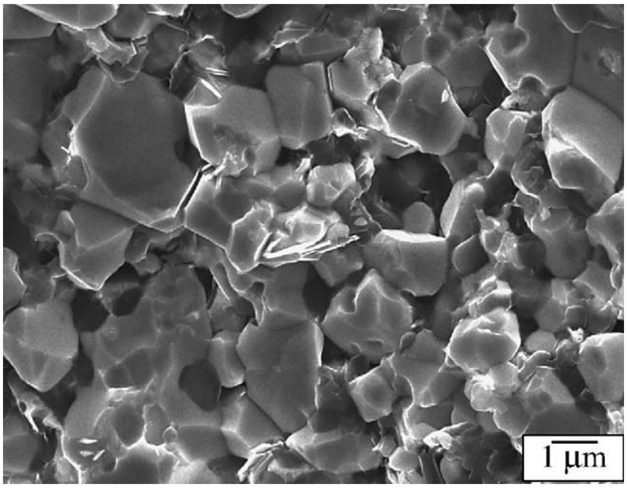

Fig. 1. SEs-SEM micrograph of a fracture surface.